Research Article

Supplementary Information

Catalytic Gold Nanostars for SERS-based Detection of Mercury Ions (Hg^{2+}) with Inverse Sensitivity

Natasha Logan,[1†] Javier Lou-Franco,[1†] Christopher Elliott,[1] and Cuong Cao,[1,2,*]

[1]Institute for Global Food Security, School of Biological Sciences, Queen's University of Belfast, 19 Chlorine Gardens, Belfast, BT9 5DL, UK.

[2]Material and Advanced Technologies for Healthcare, Queen's University of Belfast, 18-30 Malone Road, Belfast, BT9 5BN, UK.

* Corresponding author. Email: c.cao@qub.ac.uk

† These authors contributed equally to this work

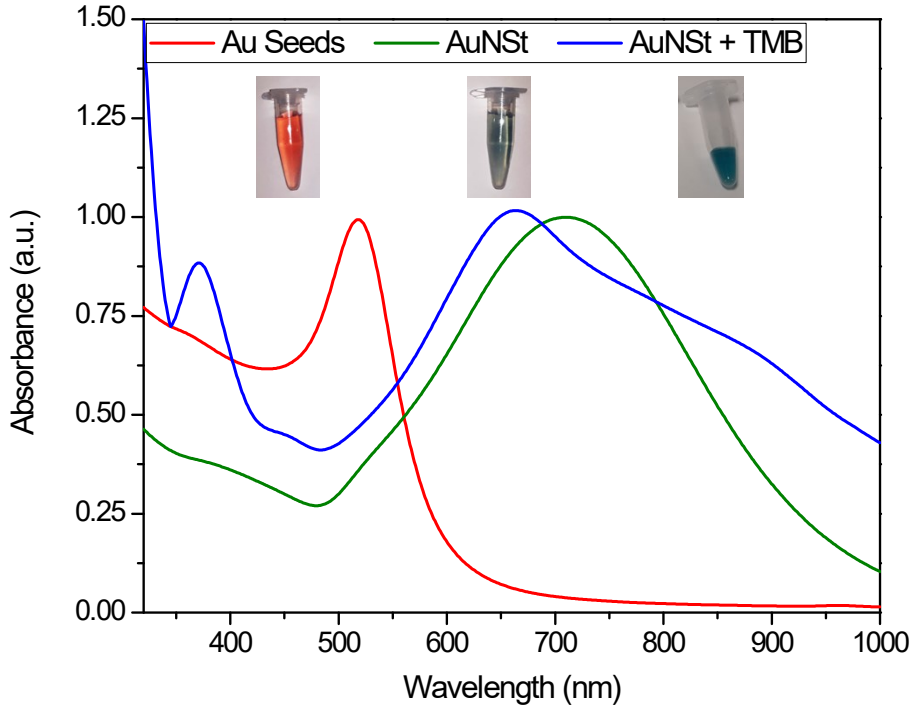

Fig. SI.1: Spectroscopic and colorimetric analysis of various colloidal solutions: gold (Au) seeds exhibiting a characteristic wine-red colour (red line and left image), gold nanostars (AuNSt) displaying a green-blue colour after synthesis (green line and middle image) and the intense blue colour generated by the oxidation of chromogenic TMB substrate due to the peroxidase-like activity of AuNSt (blue line and right image).

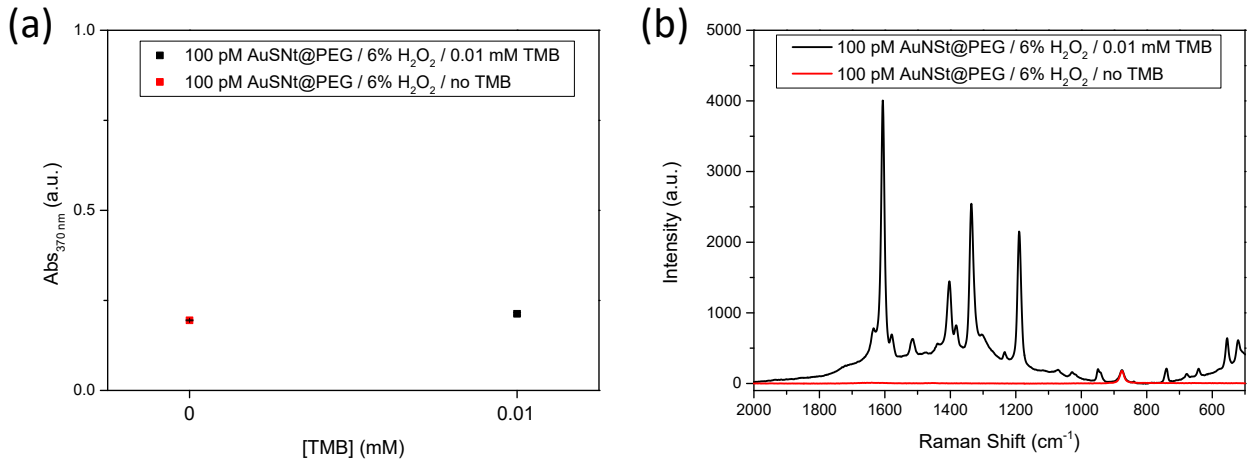

Fig. SI.2: Detection of oxTMB generated using 100 pM AuNSt-PEG with 0.01 mM TMB in an aqueous solution containing 6% H_2O_2. (a) UV-Vis analyses measuring $A_{370\ nm}$ after 20 min of reaction of AuNSt in the presence of a minimal concentration of TMB and in the absence of TMB (negative control). The samples are analysed in triplicate. (b) Raman spectroscopy analyses of the same samples analysed by UV-Vis spectroscopy. Raman measurements were performed using a laser power of 20 mW, wavelength source 785 nm, 10 exposures with an integration time of 5 s and a 10x objective lens.

UV-Vis and Raman spectroscopy analyses were performed to show the sensitivity of each approach as a detection mechanism to measure oxTMB. A TMB concentration small enough (0.01 mM) was added to 100 pM AuNSt-PEG in a 6% H_2O_2 aqueous solution to generate oxTMB. The samples were prepared in triplicate and showed a signal indistinguishable from the negative control by UV-Vis spectroscopy, but a clear positive result by Raman spectroscopy. These analyses justify the need of the Raman microscope to develop the Hg sensor, since the colorimetric approach would not provide the sensitivity required for a diagnostic assay.

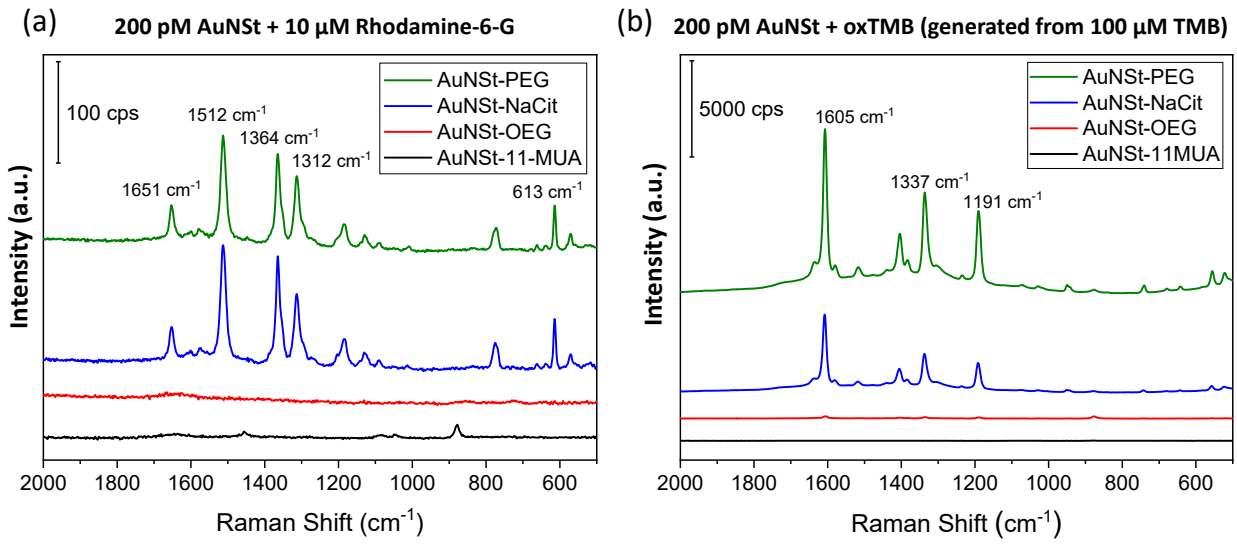

Fig. SI.3: AuNSt (200 pM) with varied surface coating moieties; PEG (cyan line), citrate (blue line), OEG (red line) and 11-MUA (black line) displaying different Raman enhancement in the presence of (a) 10 µM Rhodamine-6-G (R6G) and (b) oxTMB generated from 100 µM TMB.

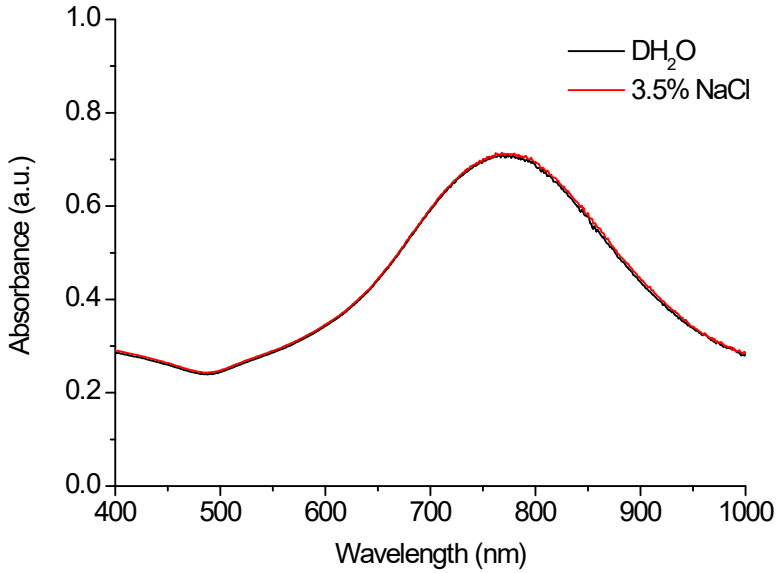

Fig. SI.4: UV-Vis spectra of functionalised AuNSt in the absence (black line) and presence (red line) of 3.5% NaCl confirming the stability of PEG-SH functionalised AuNSt ($\lambda_{max.}$= 781 nm).

AuNSt synthesised with this method use $HAuCl_4$ as a gold source, $AgNO_3$ to enhance the anisotropic growth of Au branches on certain crystallographic facets, L-Ascorbic Acid (L-AA) as a reducing agent, and Au seeds which act as nuclei during anisotropic growth, which results in the formation of branches or tips, and a star-shaped nanoparticle. To modify the size of the AuNSt, the amount of $HAuCl_4$ and/or Au seeds can be varied. Increasing the amount $HAuCl_4$ will result in a larger AuNSt, as will reducing the amount of Au seeds. Similar to spherical gold the AuNSt also requires the addition of a stabiliser, to avoid aggregation and to maintain stability in solution which takes place as a final step after synthesis.

The PEG molecule (*O*-(3-Carboxypropyl)-*O*′-[2-(3-mercaptopropionylamino)ethyl]-polyethylene glycol) was successfully functionalised to the surface of the AuNSt via strong interactions between thiol (SH) and Au, and remain stable for several weeks when stored at 4°C. The concentration of NaCl was chosen to reflect the concentration of NaCl present in seawater (3.5%), and to confirm whether the PEG-functionalised AuNSt would remain stable

in a harsh seawater matrix. The results confirm no shift in the absorption spectra between AuNSt-PEG with dH_2O (black line) and 3.5% NaCl (red line), with the typical absorption peak remaining at 781 nm. In addition, as there is a crossover between absorbance and scattering the AuNSt-PEG will be suitable for excitation with a 785 nm laser. Overall, this demonstrates the excellent stability of AuNSt-PEG, and their suitability for detecting Hg^{2+} in a wide range of high electrolyte matrices using SERS.

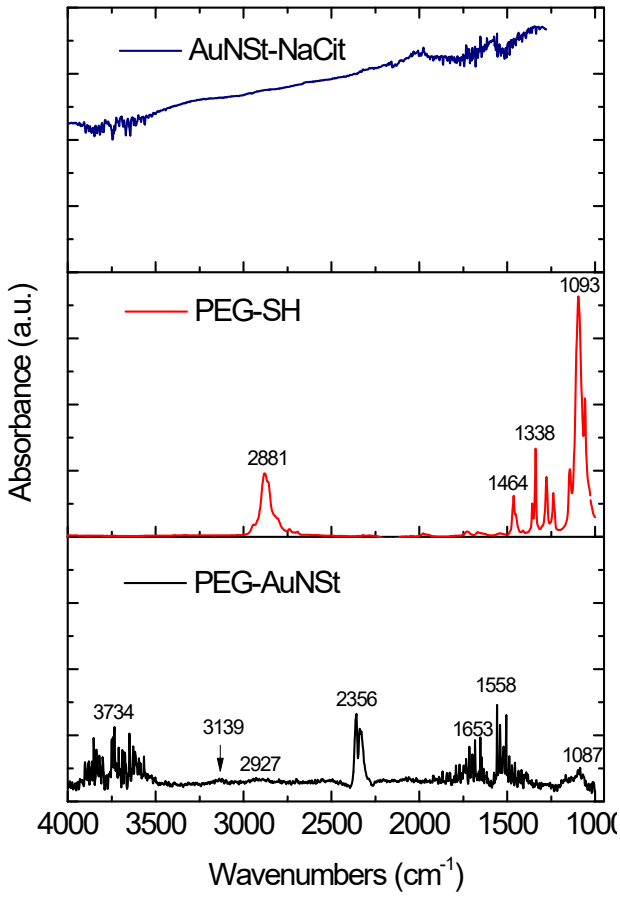

Fig. SI.5: Characterisation of AuNSt-PEG using FTIR. Spectra for bare-AuNSt with NaCit (blue line), PEG molecule (red line) and PEG-functionalised AuNSt (black line).

FTIR spectroscopy was conducted to confirm the successful functionalisation of PEG to the surface of AuNSt. The spectra for AuNSt-NaCit do not show an absorption spectrum as inorganic materials (navy line). However, the PEG-SH molecule (red line) shows strong absorption bands in similar positions to AuNSt-PEG (black line). Briefly, the bands at 1093 cm^{-1} correspond to the C-O-C bending bands of PEG [1], and are diminished after functionalisation with AuNSt, which can be seen by the small band at 1087 cm^{-1}. Other bands within the fingerprint region 1338 cm^{-1} and 1464 cm^{-1} correspond to C-H bending [2] and are shifted to 1558 cm^{-1} and 1653 cm^{-1}, respectively. The new band at 1653 $cm^{-}1$ can be attributed to C=O bending of the carboxyl groups, and these double bonds are shifted after functionalisation of PEG with the AuNSt surface, through thiol-gold interactions. The characteristic peak at 1558 cm^{-1} can be attributed to amide signal related to C-S stretching and

to the presence of the mercapto end group (PEG-SH), as discussed previously [3]. The band at 2356 cm^{-1} in the spectra of AuNSt-PEG confirms the presence of a C≡C bond, which overall confirms the strong Au-S bond between PEG-thiol and the Au surface. The bands at 2881 cm^{-1} and 2927 cm^{-1} correspond to the asymmetric and symmetric stretching of the C-H bands [2] for pure PEG-thiol and AuNSt-PEG, respectively. This band is severally diminished after functionalisation, suggesting that the C-H band is disrupted after PEG anchors onto the surface of the AuNSt, which may be attributed to the displacement of hydrogen bonds. Finally, the bands at 3139 cm^{-1} and 3734 cm^{-1} correspond to O-H and N-H stretching and may be attributed to trapped water or alcohol molecules [1]. Overall, we can verify by FTIR that the functionalisation of AuNSt with PEG was successful.

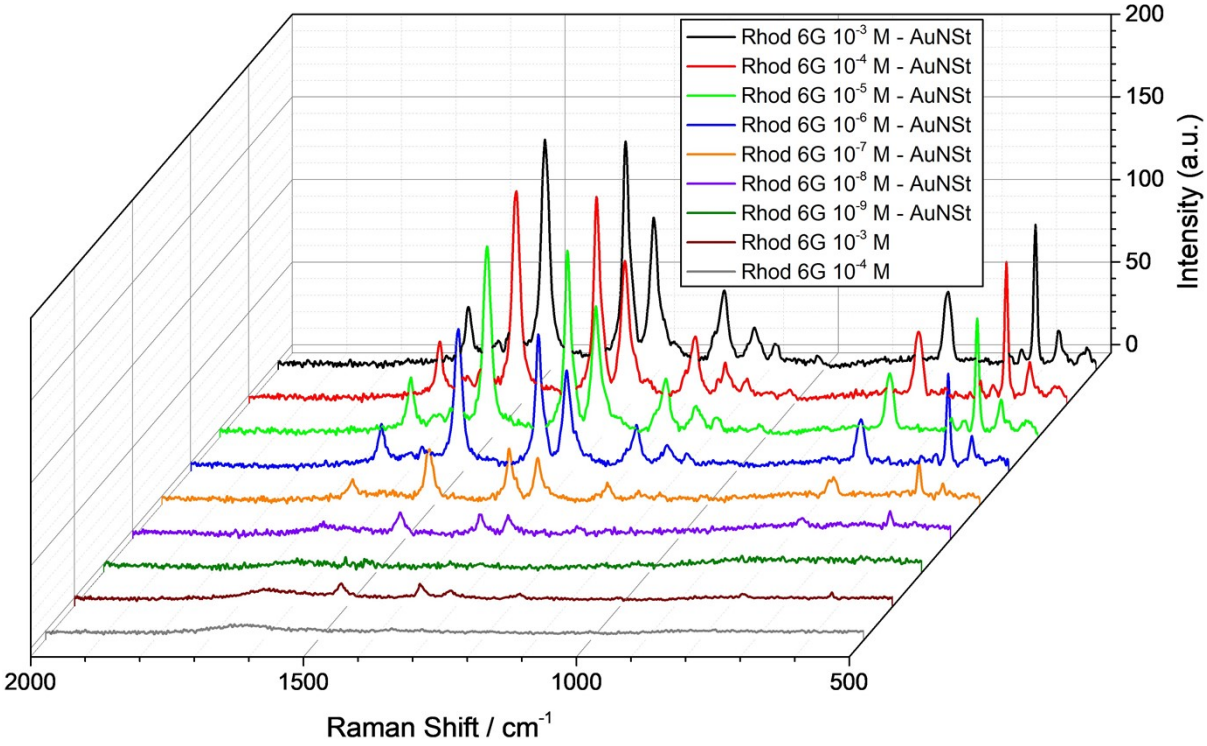

Fig. SI.6: Raman spectra of decreasing concentrations of Rhodamine 6G in the presence and absence of AuNSt.

Rhodamine 6G (R6G), a well-known Raman active molecule, has been used for characterising the potential of AuNSt as Raman enhancers. Samples containing a range of R6G concentrations from 10^{-3} to 10^{-9} M were prepared and measured in two different conditions: in the presence of 200 pM AuNSt and on their own. R6G has been described in the literature to generate two strong bands corresponding to the aromatic C – C stretch modes at 1512 and 1364 cm^{-1}. Other major peaks can be observed at 1312, 1184, 775 or 613 cm^{-1}, whose presence has already been reported and assigned in previous studies [4]. The stronger band (1512 cm^{-1}) has been used as reference to compare the intensity of the signal generated in the presence and absence of AuNSt, thus allowing us to calculate their analytical enhancement factor. The analytical enhancement factor (AEF) was defined as follows [5];

$$AEF = \frac{I_{SERS}/c_{SERS}}{I_{RS}/c_{RS}}$$

where an analyte solution with concentration (c_{RS}) generates a Raman signal (I_{RS}) under non-SERS conditions or normal Raman scattering. As opposed to the signal generated (I_{SERS}) by a certain concentration of analyte (c_{SERS}), in the presence of the AuNSt.

$$AEF = \frac{I_{SERS}/c_{SERS}}{I_{RS}/c_{RS}} = \frac{13.2/1 \cdot 10^{-8}}{6.4/1 \cdot 10^{-3}} = 2.1 \cdot 10^{5}$$

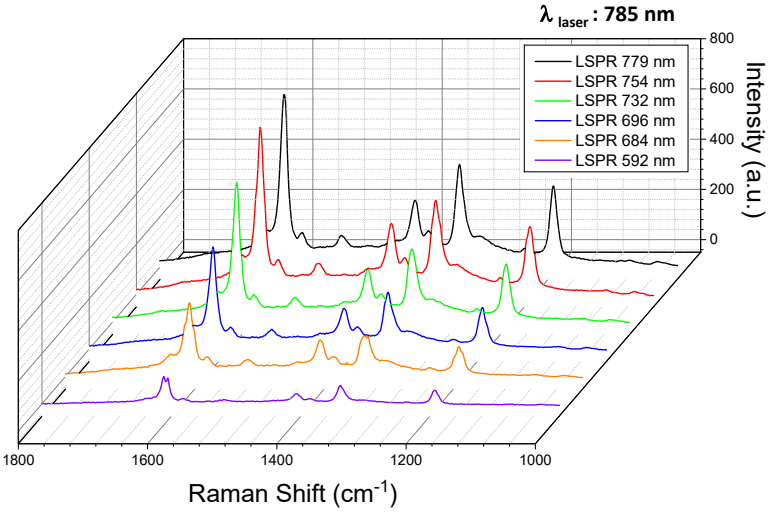

200 pM AuNSt-NaCit

0.1 mM TMB

6% H_2O_2

LSPR (nm)	$A_{370\ nm}$ (a. u.)	[oxTMB] (μM)	$SERS_{1605\ cm^{-1}}$ (cps)
779	0.378	6.1	686
754	0.415	6.7	665
732	0.397	6.4	553
696	0.435	7.1	406
684	0.452	7.3	294
592	0.560	9.1	88

Fig. SI.7: 200 pM of AuNSt-NaCit with different shapes ranging from spherical-like to star-like were mixed with 0.1 mM TMB in an aqueous solution containing 6% H_2O_2. oxTMB was measured by UV-Vis (data shown in table) and Raman spectroscopy.

Various amounts of seeds were used for the preparation of AuNSt with LSPR values distributed along the visible spectrum (from 592 to 779 nm). 200 pM of each of them stabilised with citrate were incubated with 0.1 mM of TMB in an aqueous solution containing 6% H_2O_2 to generate a fixed concentration of oxTMB (7±1 μM). These solutions were subsequently analysed by Raman spectroscopy to characterise the suitability of each AuNSt solution to act as Raman enhancers. The results showed that the closer the LSPR value got to the wavelength of the excitation source, the higher the Raman signal generated, despite oxTMB being detected in all six samples. Therefore, it can be concluded that the less spherical-like the AuNSt are, the better they perform in this specific analysis.

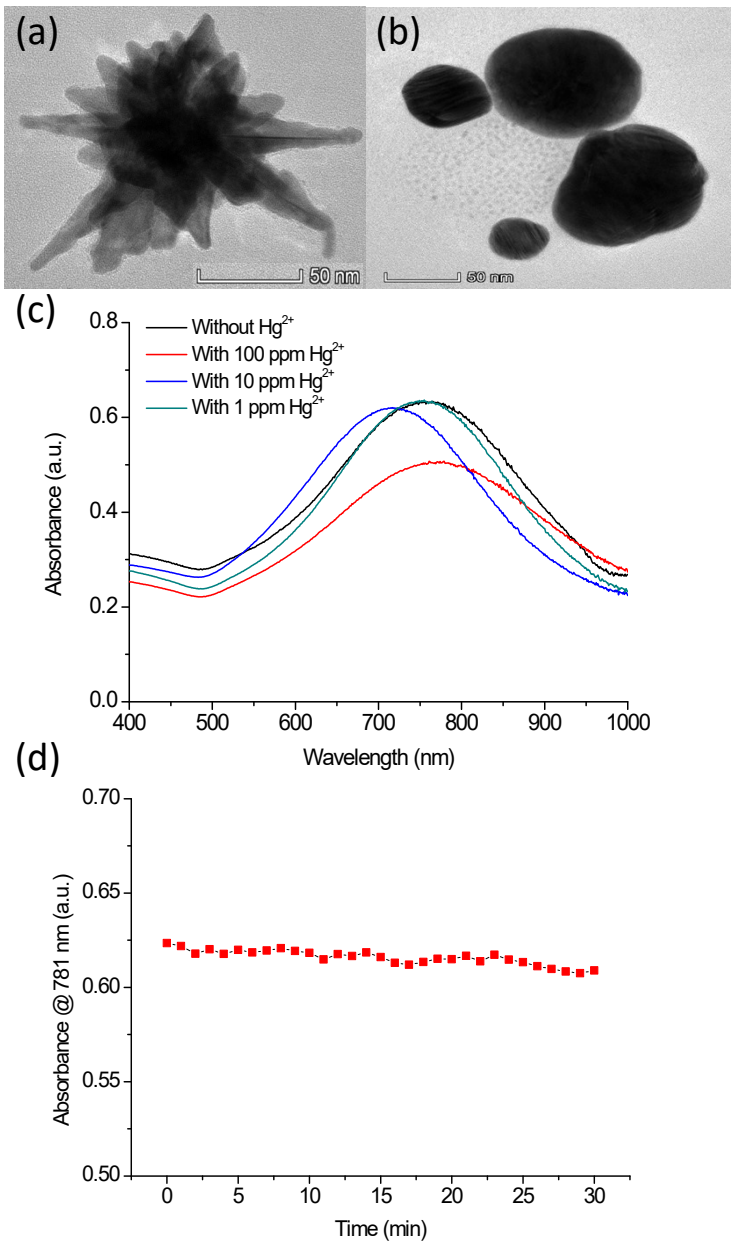

Fig. SI.8: Characterisation of AuNSt-PEG stability in the absence and presence of Hg^{2+}. (a) HRTEM image of AuNSt-PEG without Hg^{2+}. Scale bar 50 nm. (b) HRTEM image of AuNSt-PEG with 100 ppm Hg^{2+} ions. Scale bar 50 nm. (c) UV-vis spectra of AuNSt-PEG with dH_2O (black line), 100 ppm, 10 ppm and 1 ppm Hg^{2+} ions (red line, blue line, cyan line, respectively) after 10 min incubation at room temperature. (d) Kinetic analysis of AuNSt-PEG peak absorbance at 781 nm in the presence of 10 ppm Hg^{2+} ions over a 30 min incubation at room temperature.

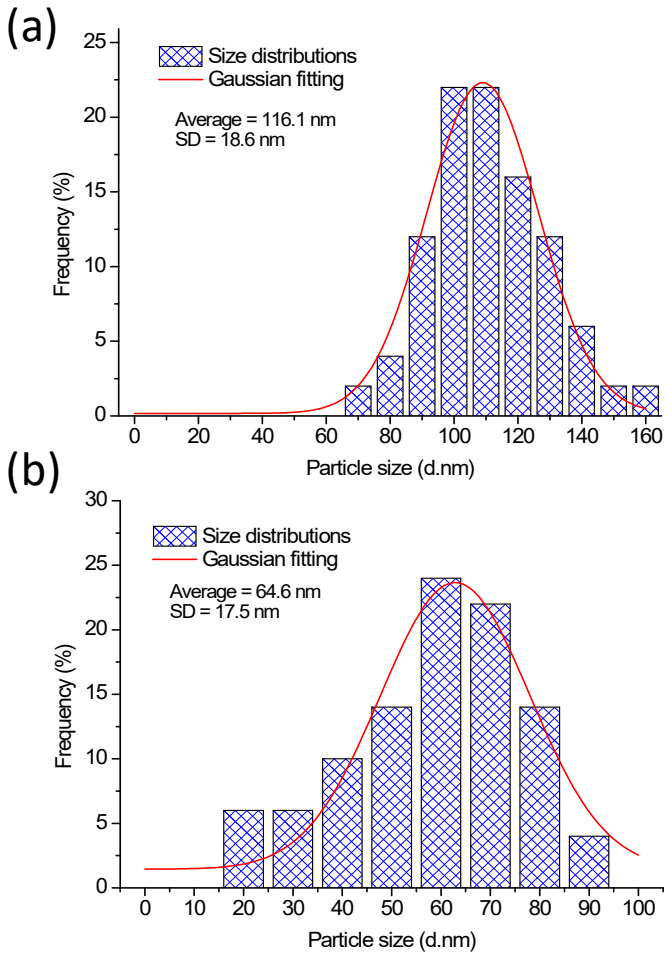

Fig. SI.9: Size distribution analysis of AuNSt-PEG in the (a**)** absence and (b**)** presence of Hg^{2+} ions with Gaussian fittings. HRTEM images (as shown in Fig. S5. a and b) were analysed and measured using Image J software. The average size (nm, *n*=50) of AuNSt-PEG and corresponding standard deviations (nm, *n*=50) were calculated as 116 nm ± 18.6 nm and 65 nm ± 17.5 nm in the absence and presence of 10 ppm Hg^{2+} ions, respectively.

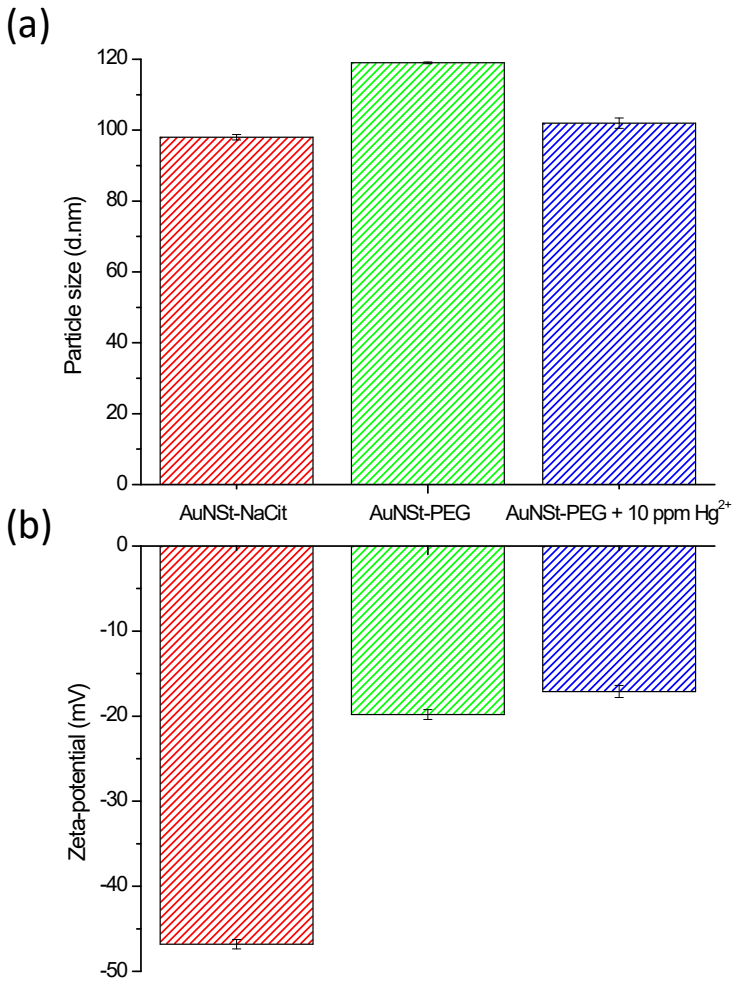

Fig. SI.10: Size and surface charge analysis of AuNSt with different surface coatings in the absence and presence of 10 ppm Hg^{2+}. (a**)** Dynamic Light Scattering (DLS) illustrating particle size and standard deviation (n=3). (b) Zeta-potential illustrating particle surface charge and standard deviation (n=3) for AuNSt-NaCit (red stripe), AuNSt-PEG (green stripe) and AuNSt-PEG in the presence of 10 ppm Hg^{2+} (blue stripe).

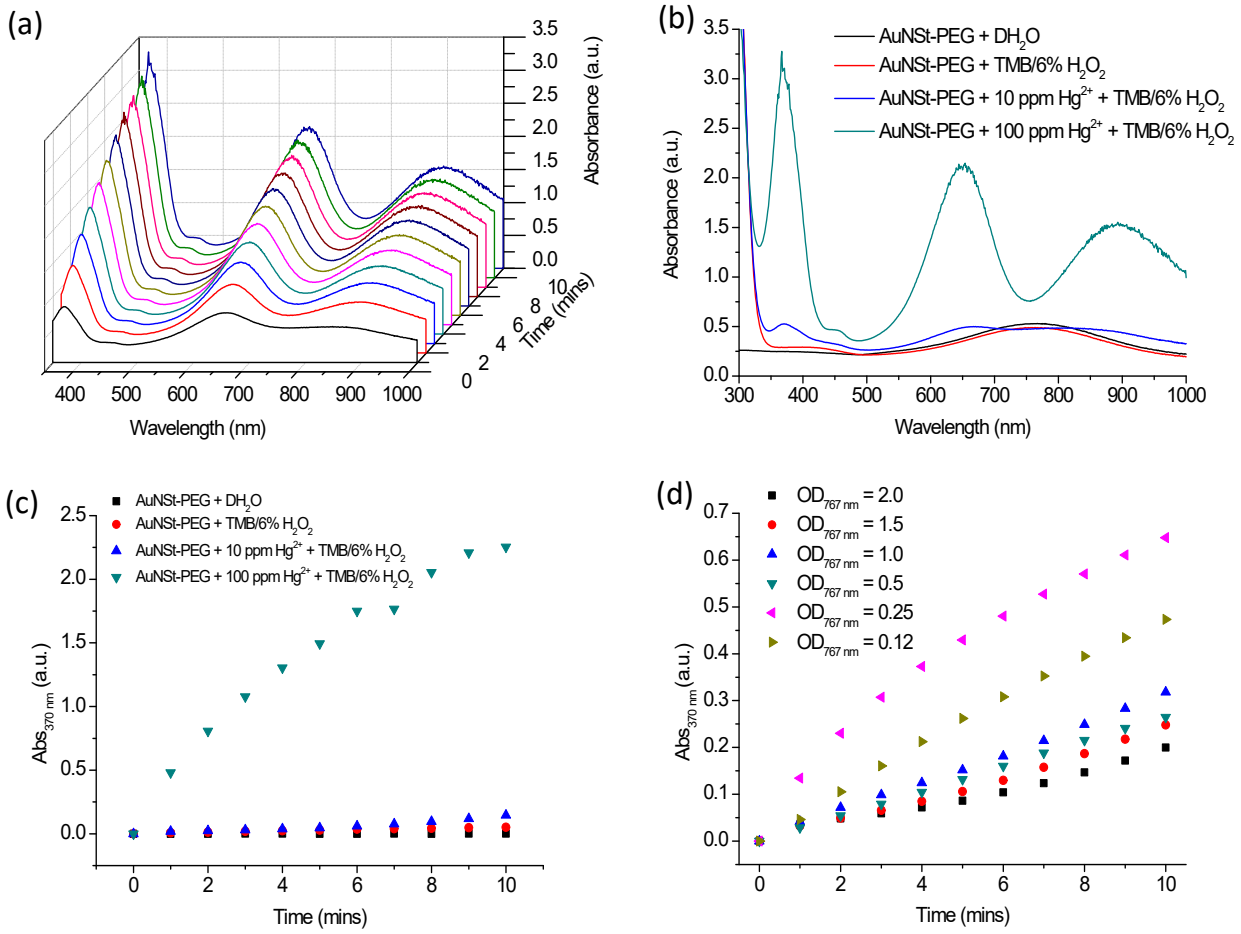

Fig. SI.11: Ultraviolet-visible (UV-Vis) spectroscopy of AuNSt-PEG ($OD_{767\ nm}$ = 2.5) in the presence of Hg^{2+} ions and 1.25 mM TMB with 6% H_2O_2. (a) Waterfall graph displaying full wavelength kinetics over 10 min confirming enhanced oxidation of TMB substrate in the presence of 100 ppm Hg^{2+}. (b) Full wavelength spectra after 10 min confirming improved catalytic activity of AuNSt-PEG in the presence of 100 ppm Hg^{2+} (cyan line), in comparison to AuNSt-PEG alone (red line). (c) Kinetic analysis over 10 min illustrating improved reaction rates for TMB oxidation in the presence of AuNSt-PEG and 100 ppm Hg^{2+} (cyan triangles) however, also confirming reduced reaction rates in the presence of 10 ppm Hg^{2+} (blue triangles). (d) Optimisation of AuNSt-PEG concentration confirms the recovery of catalytic activity in the presence of 10 ppm Hg^{2+}.

The results can confirm that the catalytic activity of AuNSt-PEG can be greatly improved by the presence of Hg^{2+} ions. Thus, Au-Hg amalgamation can help to facilitate the catalytic reaction and oxidation of TMB substrate to an oxidised blue-coloured product.

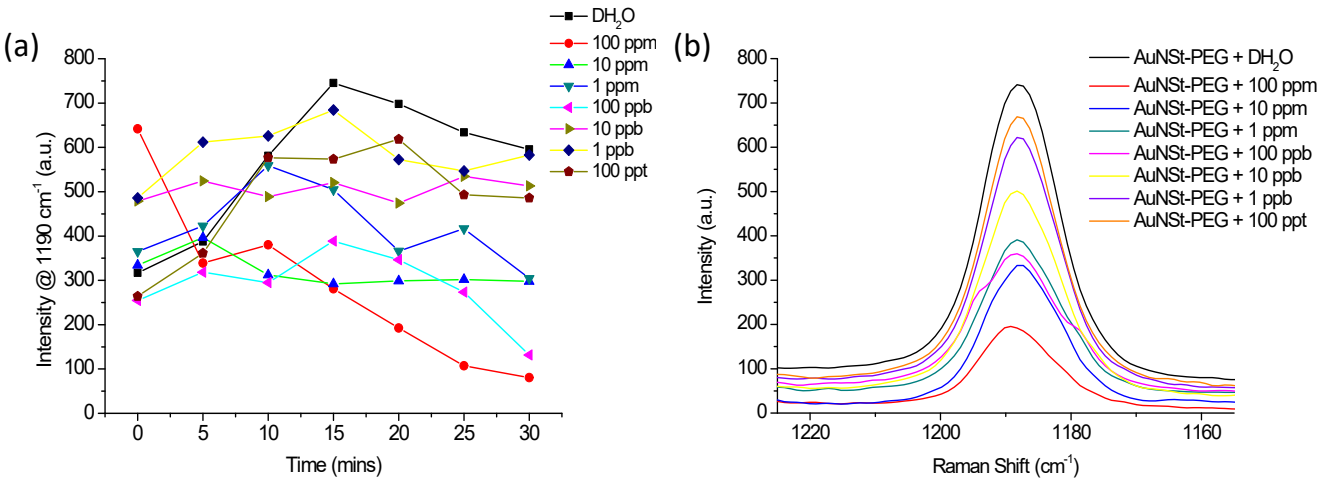

Fig. SI.12: Optimisation of AuNSt-PEG assay parameters. (a**)** Kinetic analysis over 30 min for AuNSt-PEG ($OD_{781\ nm}$=3.0) in the presence of different Hg^{2+} ion concentrations ranging from 0-100 ppm and 1.25 mM TMB with 6% H_2O_2, at a fixed SERS intensity of 1190 cm^{-1}. (b**)** SERS intensity of oxTMB peak at 1190 cm^{-1} after 20 min incubation at room temperature, showing a linear correlation between decreasing SERS intensity and increasing Hg^{2+} ion concentration.

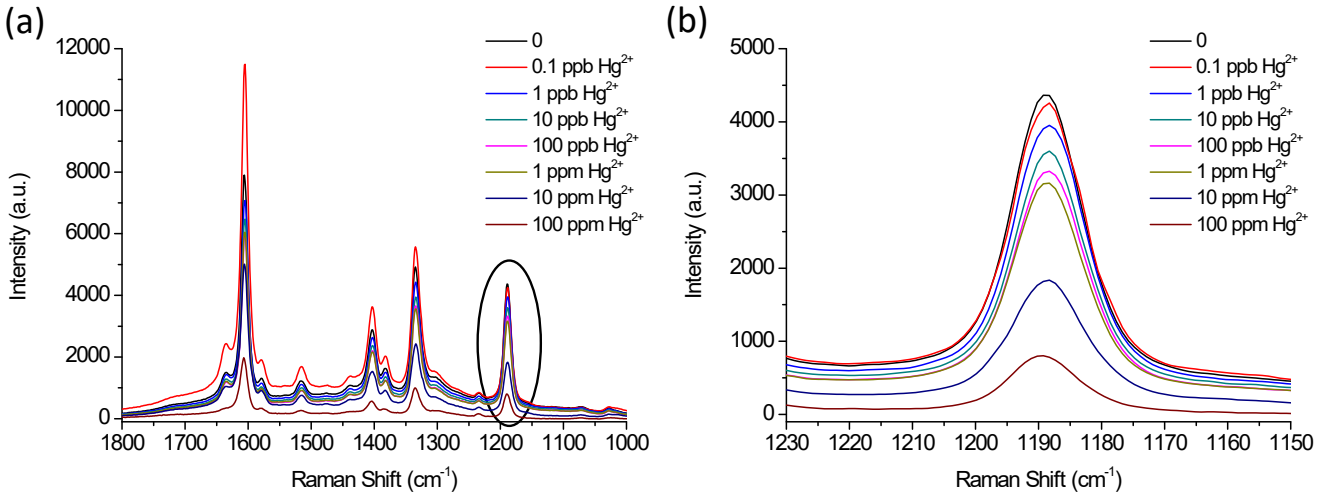

Fig. SI.13: SERS intensity of AuNSt-PEG in the presence Hg^{2+} ions analysed in a coastal seawater Hg^{2+} Certified Reference Material (CRM) to demonstrate the sensitivity and applicability of the sensing mechanism. (a**)** Full SERS spectra of AuNSt-PEG with increasing Hg^{2+} concentrations highlighting spectral features of oxTMB. (b**)** Analysis of oxTMB band at 1190 cm^{-1} (black circle in a).

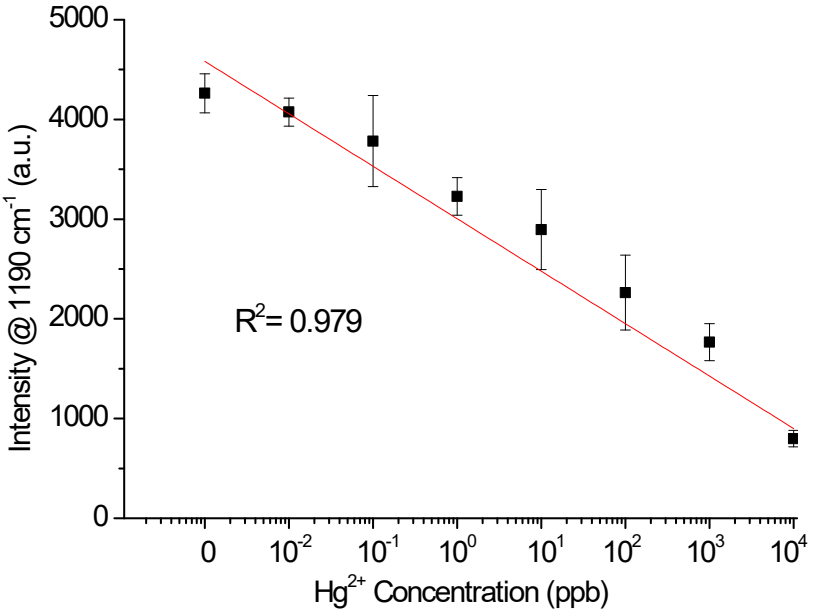

Fig. SI.14: Linear relationship between spiked Hg^{2+} concentration and decreasing SERS intensity at 1190 cm^{-1} for AuNSt-PEG analysed in a coastal seawater Hg^{2+} Certified Reference Material (CRM) (R^2=0.979)

Supplementary references

1. C. Cao, S.J. Sim, Preparation of highly stable oligo(ethylene glycol) derivatives-functionalized gold nanoparticles and their application in LSPR-based detection of PSA/ACT complex. *J. Nanosci. Nanotechnol*., 2007, **7**(11), 3754-3757.
2. K. Shameli, M.B. Ahmad, S.D. Jazayeri, S. Sedaghat, P. Shabanzadeh, H. Jahangirian, M. Mahdavi, Y. Abdollahi, Synthesis and characterization of polyethylene glycol mediated silver nanoparticles by the green method. *Int. J. Mol. Sci*., 2012, **13**(6), 6639-6650.
3. E. Keleş, B. Hazer, F.B. Cömert, Synthesis of antibacterial amphiphilic elastomer based on polystyrene-block-polyisoprene-block-polystyrene via thiol-ene addition. *Mater. Sci. Eng. C*., 2013, **33**(3), 1061-1066.
4. L. Jensen, G.C. Schatz, Resonance raman scattering of rhodamine 6G as calculated using time-dependent density functional theory. *J. Phys. Chem. A*., 2006, **110**(18), 5973-5977.
5. E.C. Le Ru, E. Blackie, M. Meyer, P.G. Etchegoin, Surface enhanced raman scattering enhancement factors: A comprehensive study. *J. Phys. Chem. C*., 2007, **111**(37), 13794-13803.